Powder Technology 333 (2018) 293–303

Contents lists available at ScienceDirect

Powder Technology

journal homepage: www.elsevier.com/locate/powtec

Flow regimes in gas-liquid-solid mini-fluidized beds with single gas orifice

Yanjun Li [a], Mingyan Liu [a,b,*], Xiangnan Li [a]

[a] Collaborative Innovation Center of Chemical Science and Engineering (Tianjin), School of Chemical Engineering and Technology, Tianjin University, Tianjin 300350, China
[b] State Key Laboratory of Chemical Engineering (Tianjin University), Tianjin 300350, China

ARTICLE INFO

Article history:
Received 18 September 2017
Received in revised form 5 February 2018
Accepted 14 April 2018
Available online xxxx

Keywords:
Gas-liquid-solid
Fluidization
Mini-fluidized bed
Flow regime
Wall effect

ABSTRACT

Flow regimes and their transitions in the gas-liquid-solid mini-fluidized beds (MFBs) with single gas orifice were studied experimentally in this paper. The diameter of the fluidized beds varied from 3 mm to 5 mm and the vertical column height was 50 mm. The ranges of superficial gas velocity and liquid velocity were 1.96×10^{-4}–4.73×10^{-3} m/s and 5×10^{-6}–4.2×10^{-2} m/s, respectively. The solid particles ranged in size from 50 μm to 300 μm. Half-fluidization, slug, dispersed bubble and transport flow regimes in the three-phase MFBs were identified by analyzing minimum fluidization velocity, pressure drop, and entrainment velocity of solid particles based on experimental data of pressure drop and fluidization velocity as well as flow observations. The effects of solid particle, liquid properties, bed, gas orifice sizes, and static bed height on the flow regimes and transitions were investigated. Results showed that the behavior of gas bubbles and the wall effect affected the flow regimes and transitions. Obvious wall effect increased minimum fluidization liquid velocity in the liquid-solid mini-fluidized beds, which increased the transition liquid velocity from the half-fluidization to slug flow regimes. Moreover, wall effect made Taylor bubbles bigger at lower superficial liquid velocities due to the bubble coalescence and the transition boundaries expansion. Solid particles aggregation, wall effect and bubble wake behavior were responsible for increment of the minimum entrainment velocity of solid particles. Flow regime maps of the gas-liquid-solid MFBs were presented and correlations were suggested for the flow regime boundaries.

1. Introduction

Gas-liquid-solid fluidized beds are widely used in the industrial processes [1]. The identification of three-phase flow regimes and their transitions is a fundamental topic and requires further investigations. Related researches have been reported in previous literatures [2–5].

Several techniques have been adopted to study the flow regimes and their transitions, such as visual observation [2,4–7], pressure fluctuation analysis [6] and measurement of local hydrodynamics with various probes [8,9]. Specifically, probe technique can be used to detect the local characteristics of the multiphase flow, and then flow regime can be inferred based on the statistical parameters or other indicators derived from probe output signals.

For example, Lee et al. [10] tried to correlate the flow regimes and their transitions with the properties of gas bubbles and gas holdup that could characterize the flow hydrodynamics in the gas-liquid-solid fluidized beds. Zhang et al. [11] developed a measurement method and criteria based on gas bubble or gas holdup characteristics covering very broad operational ranges for gas and liquid phases. Correlations based on these criteria were provided to predict the flow regime transitions in the gas-liquid-solid fluidized beds. Recently, Abbasi et al. [12] and Sheikhi et al. [13] used the non-intrusive vibration signals acquired from accelerometers to investigate the hydrodynamics in the gas-liquid-solid fluidized beds. The minimum fluidization velocity was confirmed from the analysis of vibration signals. The bubble regime transitions in the three-phase fluidized beds were obtained according to the average cycle frequency of vibration fluctuations. Furthermore, Omid Arjmandi-Tash et al. [14,15] applied time series analysis techniques in time and frequency domains, and S statistics method to characterize three-phase fluidization. In this way, they detected four distinct fluidization regimes and revealed the existence of transition velocities.

With the development of the manufacturing techniques of microstructures, micro-channel devices are gaining interest and becoming relevant to chemical and biological applications [16]. In micro-channel, the surface tension, inertia and the viscosity are predominant, while buoyancy is suppressed and the flow is independent of channel orientation with respect to gravity. Therefore, two-phase flow regimes of micro-channel are different from those of larger channels [17–22].

For example, Triplett et al. [23] observed gas bubble flow, slug flow, slug-annular flow and annular flow in circular micro-channels with 1.1

* Corresponding author at: School of Chemical Engineering and Technology, Tianjin University, Tianjin 300350, China.
E-mail address: myliu@tju.edu.cn. (M. Liu).

https://doi.org/10.1016/j.powtec.2018.04.029
0032-5910/

and 1.45 mm inner diameters, and in micro-channels with semi-triangular cross-sections with hydraulic diameters of 1.09 and 1.49 mm. They found that relevant flow regime models and correlations in larger channels did not apply to micro-channels. The results of Chen et al. [24] were similar to those of Triplett et al. [23]. Bubble-train slug flow occurred instead of slug-annular flow in their work. Serizawa et al. [25] found gas bubble flow, slug flow, liquid ring flow, liquid lump flow, annular flow, frothy or wispy annular flow, rivulet flow, liquid droplets flow and skewed flow for air-water flow in circular tubes of 20, 25 and 100 μm i.d. and for steam-water flow in a 50 μm i.d. circular tube. In addition, Akbar et al. [26] and Waelchli and von Rohr [27] proposed the entire flow regime maps based on appropriate dimensionless parameters.

The mini-fluidized beds (MFBs) are miniaturized products of conventional fluidized beds [28–30] and have been applied for analyses of kinetics and mechanism [31–33], biomass pyrolysis [34], gasification [35–38] and photo catalytic activity [39]. Wang and Fan [40] studied on the flow regimes in gas-solid MFBs with the bed diameter of 0.7–5 mm. They found that the instability of flow regime transition appeared in the 700 μm and 1 mm channels. When the gas velocity was beyond the minimum fluidization velocity (U_{mf}), the flow regime underwent from bubble/slug flow to particulate fluidization at a given gas velocity, which was different from the fluidization in a larger bed. The differences of flow regimes cause the discrepancies of fluidization quality, performance of phases contacting, mass and heat transfer rates, production efficiency and other aspects. Therefore, characterizing and classification of flow regimes are very important and basic tasks in studying the fluidized beds. For the miniaturized fluidized beds, wall obviously affects phase interaction leading to differences in hydrodynamic behavior. However, no effort has been made to detect dominant flow structures with wall effect in the gas-liquid-solid MFBs.

This study will address the flow regimes and their transitions with wall effect in the gas-liquid-solid MFBs through the visual observation and pressure fluctuation analysis. This will widen the knowledge on the hydrodynamic behavior of these types of fluidized beds. The transition points between different flow regimes were identified based on the fluidization experiments with the bed diameter of 3–5 mm. Furthermore, correlations that can be used to predict the flow regime transitions were proposed.

2. Experiment and method

The main component of the experimental setup consisted of a column made of polymethyl methacrylate (PMMA) with column diameter of 3 mm and height of 50 mm, as is shown in Fig. 1. The configuration was described in Li et al. [30]. Air and deionized water or other liquid phases (listed in Table 1) were used as the gas and liquid phases, respectively. The flow rates of gas and liquid phases were controlled by the syringe pumps. The superficial gas velocity ranged from 1.96×10^{-4} to 4.73×10^{-3} m/s, while the superficial liquid velocity varied from 5×10^{-6} to 4.2×10^{-2} m/s. Five types of solid particles were used and their properties were shown in Table 2. The size distribution of solid particles was measured with a Rise 3000 Laser Size Measuring Apparatus (Rise Size Measurement Co. Ltd., China) at a measurement range of 0.1 to 3500 μm.

For all fluidization experiments, the bed dynamic pressure drop of solid particles (where the hydrostatic head of liquid phase is subtracted due to the measurement method) was calculated by:

$$\Delta P_f = \Delta P_t - \Delta P_e \tag{1}$$

where, ΔP_f, ΔP_t and ΔP_e are the bed pressure drop of solid particles, total pressure drop and pressure drop of empty beds including the distributor pressure drop, respectively. At least three times of experiments were conducted in a given set of operation conditions.

Standard deviation of the pressure drop series is a measure of the data set dispersion from its average. A higher deviation of data from the mean value leads to a higher standard deviation. This parameter is defined as.

$$\sigma' = \sqrt{\frac{1}{N-1}\sum_{n-1}^{N}(x(n)-\overline{x})^2} \tag{2}$$

where,

$$\overline{x} = \frac{1}{N}\sum_{n=1}^{N} x(n) \tag{3}$$

Verification of the measured pressure drop was shown in Li et al. [30].

A complementary metal-oxide-semiconductor transistor (CMOS) high speed camera (A504k, Basler Vision Technology Co. Ltd., German) with a microscopic magnification lens (AT-X M-100 PROD, Kenko Tokina Co. Ltd., Japan) was used to capture the dynamic image of gas bubbles in the three-phase bed. Bubble sizes were analyzed by using image analysis software of Image J (National Institutes of Health, United

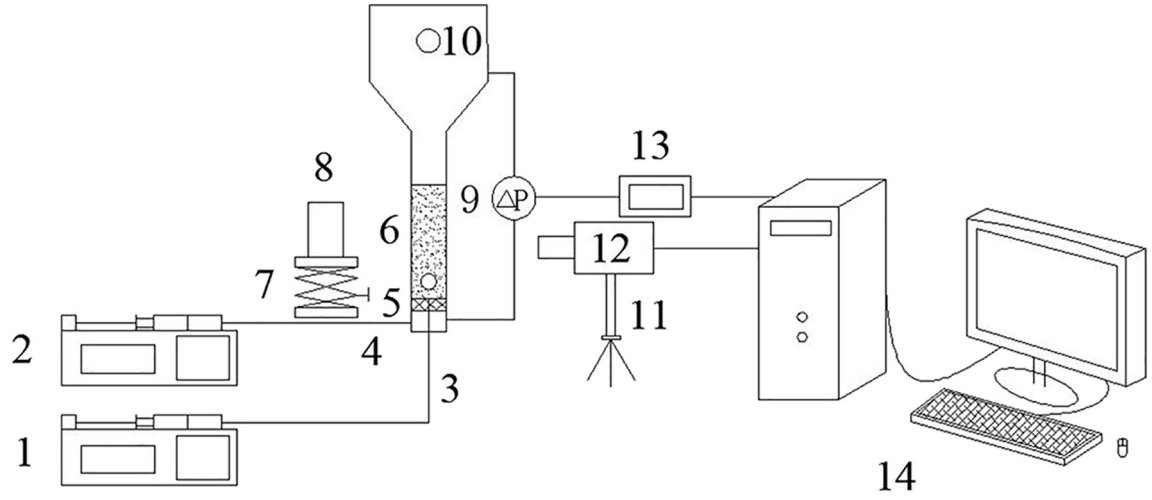

Fig. 1. Schematic diagram of the gas-liquid-solid MFBs. (1) Gas syringe pump; (2) liquid syringe pump; (3) gas inlet; (4) liquid inlet; (5) liquid distribution; (6) test section; (7) lifting platform; (8) cold light source; (9) pressure transducer; (10) outlet; (11) tripod; (12) CMOS camera; (13) A/D converter; (14) computer.